Biodistribution and Imaging of FDG in Rats with LS174T Carcinoma Xenografts and Focal *Escherichia coli* Infection

Peter J.M. Kok, Juliëtte E.M. van Eerd, Otto C. Boerman, Frans H.M. Corstens, and Wim J.G. Oyen
Department of Nuclear Medicine, Radboud University Nijmegen Medical Center, Nijmegen, The Netherlands

ABSTRACT

Objective: *The aim of this study was to compare the dynamic distribution of fluorodeoxyglucose (FDG) in malignant and in infectious lesions.* ***Methods:*** *The dynamic distribution of FDG was studied in Rowett nude (RNU) rats with a LS174T carcinoma xenograft in the left front leg and an* Escherichia coli–*induced focal infection in the right front leg. In 5 rats, dynamic FDG-PET was performed (27 frames of 6–15 minutes) up to 4 hours after injection of 11 MBq* ^{18}*FDG. The mean FDG uptake (SUV) was calculated and plotted by using a region of interest (ROI) centered over both lesions. In groups of 6 rats, the biodistribution of FDG was determined by counting dissected tissues at 1, 2, 3, and 4 hours after an injection of 11 MBq FDG. Means* ± *the standard error of the mean (SEM) were calculated.* ***Results:*** *Dynamic positron emission tomography (PET) visualized both the tumor and the infection. The ROI analysis showed that FDG uptake in the infections was faster and higher, as compared to the tumor lesions. FDG uptake in the tumor reached a standardized uptake value (SUV) of 0.8* ± *0.3 at 60 minutes and in the infectious lesions a SUV of 1.6* ± *0.2 at 45 minutes, both remaining constant until 4 hours postinjection (p.i.). In the biodistribution study with* ex vivo *tissue counting, FDG had accumulated up to 1.1* ± *0.1 %ID/g and 0.8* ± *0.1 %ID/g at 1 hour in the tumor and infection, respectively, and remained constant until 4 hours for both lesions without significantly different wash-out from the 2 lesions. The tumor/blood and abscess/blood ratios increased with time to 57* ± *17 and 48* ± *14, respectively.* ***Conclusion:*** *Although in this model differences in absolute FDG uptake and initial kinetics between tumor and infection were observed, the wash-out rate of FDG from the lesions was similar over time. The retention of FDG in the inflammatory lesion indicated that dual time-point imaging does not necessarily resolve diagnostic pitfalls for FDG-PET in oncology in order to discriminate between malignant tumorous and benign infectious lesions.*

Key words: PET, infection, tumor

Address reprint requests to: Peter J.M. Kok; Department of Nuclear Medicine, Radboud University Nijmegen Medical Center; P.O. Box 9101, 6500 HB Nijmegen, The Netherlands; Tel.: (+)31-243614510; Fax: (+)31-242518942; E-mail: **P.Kok@nucmed.umcn.nl**

INTRODUCTION

Fluorodeoxyglucose positron emission tomography (FDG-PET) is a sensitive modality for the diagnosis and staging of several types of malig-

nancies.[1] The accumulation of fluorodeoxyglucose (FDG) is caused by increased glucose utilization of tumor cells.[2] It has been shown that FDG also accumulates in inflammatory lesions. Lesions with a high concentration of inflammatory cells, such as granulocytes and activated macrophages, show increased uptake and retention of FDG.[3,4] High uptake of FDG in inflammatory lesions may, therefore, result in false-positive interpretations in patients with cancer, thus decreasing specificity and positive predictive value. The standardized uptake value (SUV) is not always a valid tool to distinguish between malignant and benign lesions, owing to many confounding factors, such as elevated plasma glucose level, differences in uptake period of FDG, and partial-volume effect. Recent studies have shown that FDG is better retained in malignant cells. Nakamoto et al. reported, in a study with 47 patients with suspected pancreatic carcinoma, that the retention index for malignant disease was significantly greater than that of benign disease. The addition of a later imaging time point could aid in differentiating benign and malignant lesions.[5–12]

By means of multiple time-point imaging and calculation of the SUV or lesion-to-blood ratios on both time points, it may be possible to discriminate between tumorous and infectious lesions. It has been reported that the SUV would decrease over time in case of infection, but increase or remain stable in case of malignancy.[5–12]

The aim of this study was to determine whether there are differences in the kinetics of FDG uptake between malignant and infectious lesions in a rat model.

METHODS

Preparation of Animals

All animal experiments were approved by the local animal welfare committee and performed in accordance with their guidelines. In male Rowett nude (RNU) rats (Charles River; Sulzfeld, Germany), 6–8 weeks of age with an average weight of 200 g, tumors were induced by a subcutaneous injection of 2.5×10^6 LS174T cells in the left front leg (1.25×10^7 cells/mL) 2 weeks prior to FDG injection.

The human colorectal carcinoma cell line LS174T was obtained from the American Type Culture Collection (Rockville, MD). LS174T is a rapidly growing, moderately to well-differenti-

ated human colorectal carcinoma cell line. LS174T was cultured and maintained as a confluent, growing cells on plastic in RPMI-1640 medium (GIBCO, BRL Life Science Technologies, Breda, The Netherlands), supplemented with 10% fetal calf serum (FCS) (GIBCO), L-glutamine, penicillin (100 U/mL), and streptomycin (100 μg/mL) (GIBCO, BRL Life Science Technologies).[13] Before inoculation, tumor cells were washed with 0.9% NaCl, disaggregated with 0.25% trypsin, and resuspended in complete medium to the appropriate concentration.

After 2 weeks, when tumors were approximately 1–2 cm in diameter, a soft tissue infection was induced in the right front leg by intramuscular injection of 0.2 mL *Escherichia coli* suspension (1.4×10^{10} cfu/mL).

The next day, the rats were fasted for 4 hours to avoid the influence of increased insulin and/or serum glucose levels on FDG uptake[14] and injected with 11 MBq of FDG intravenously (i.v.) (Tyco-Mallinckrodt Healthcare; Petten, The Netherlands) through the tail vein.

FDG-PET

Five RNU rats were kept anasthesized by isoflurane/nitrous oxide/oxygen inhalation. 3D PET (ECAT-EXACT, Siemens/CTI; Knoxville, TN) was performed immediately after FDG injection for a continuous period of 4 hours (27 frames of 6–15 minutes). During this period, the temperature was kept constant by a controlled external heat source to avoid temperature-dependent changes of the FDG uptake in tumor and inflammation.

The data were reconstructed and corrected for attenuation using the iterative ordered-subsets expectation-maximization (OSEM) algorithm. Images were analyzed quantitatively by drawing regions of interests (ROIs) centered over the infected tissue and the tumor without correction for partial volume effects.

The mean amount of activity, expressed as the SUV, was calculated.

Biodistribution

Groups of 6 rats were killed and dissected at 1, 2, 3, and 4 hours after FDG injection. Blood samples, abscess, and tumor were collected. The dissected tissues were weighed, and the activity in the samples was measured in a well-type gamma-counter. To correct for radioactive decay, a 1%
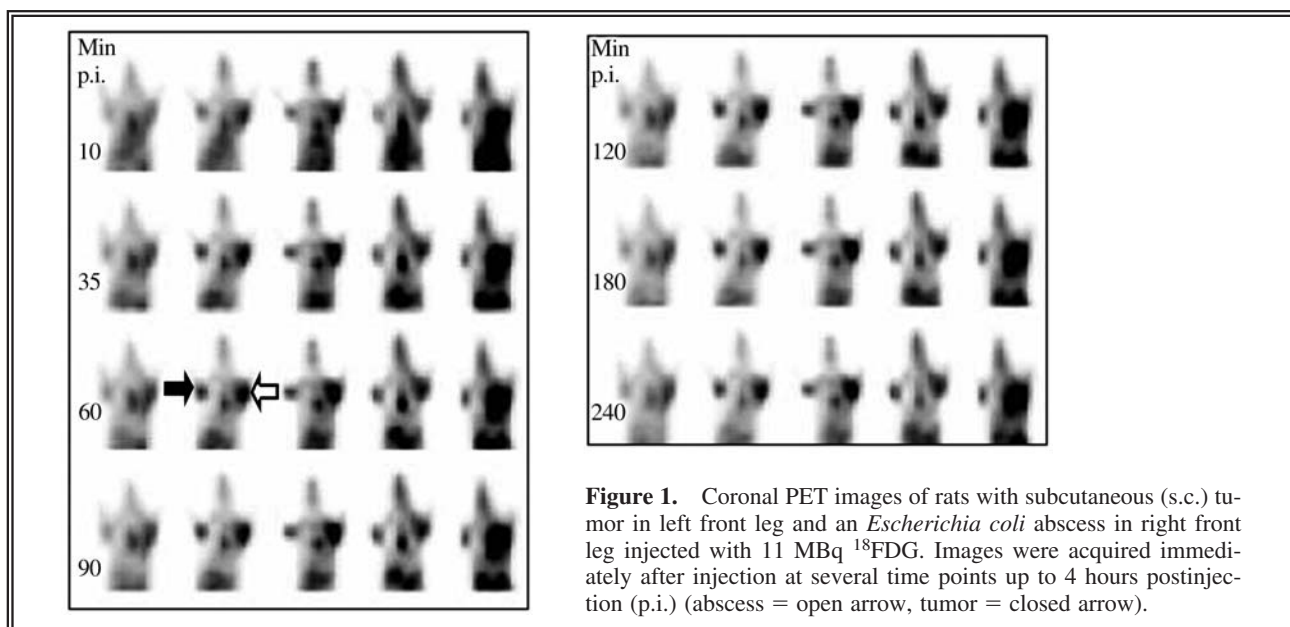
Figure 1. Coronal PET images of rats with subcutaneous (s.c.) tumor in left front leg and an *Escherichia coli* abscess in right front leg injected with 11 MBq ^{18}FDG. Images were acquired immediately after injection at several time points up to 4 hours postinjection (p.i.) (abscess = open arrow, tumor = closed arrow).

FDG standard was measured simultaneously. The activity in samples was expressed as the percentage of injected dose per gram of tissue (%ID/g). Abscess-to-blood, tumor-to-blood, and tumor-to-abscess ratios were calculated for each time point.

Statistical Analysis

All mean values are given as the mean ± one standard error of the mean (SEM). The data were analyzed statistically using a paired, two-tailed t test (GraphPad Instat 3.00 Win 95; San Diego, CA)

RESULTS

Imaging

Coronal FDG-PET images up to 4 hours are shown in Figure 1. Already at 10 minutes p.i., both the abscess and the tumor were visualized. The visualization of both lesions improved with time. Figure 2 shows the quantitative ROI analysis of the PET images. There is a fast accumulation of activity in both lesions within the 1st hour after injection, after which the uptake remains stable during the next 3 hours. The increase of the FDG uptake in the infection was significantly faster in the abscess (maximal SUV_{mean} 1.6 ± 0.03%) reached at 45 minutes; slope, 0.008 ± 0.002), as compared to the FDG uptake

in the tumor (maximal SUV_{mean} of 0.8 ± 0.3% reached at 60 minutes; slope, 0.004 ± 0.003) ($p < 0.05$). There was no washout of activity observed in either of the lesions.

Biodistribution

The results of the biodistribution at 1 hour and 4 hours p.i. are summarized in Figure 3. FDG up-
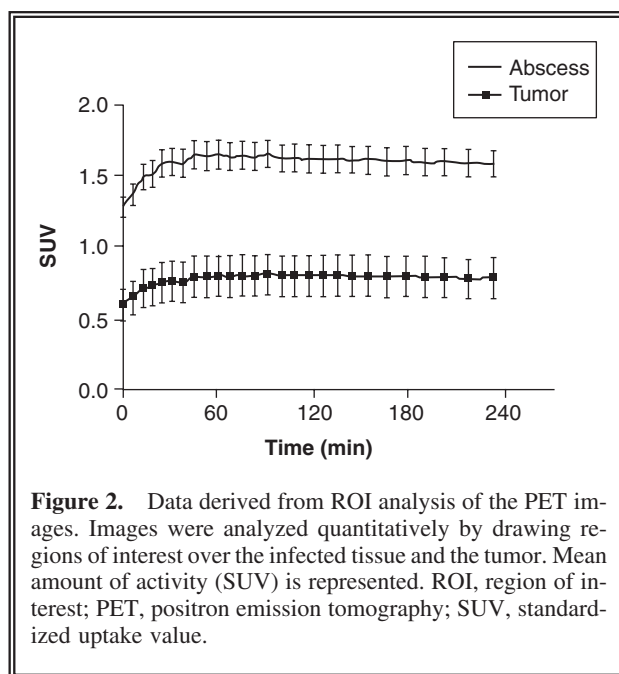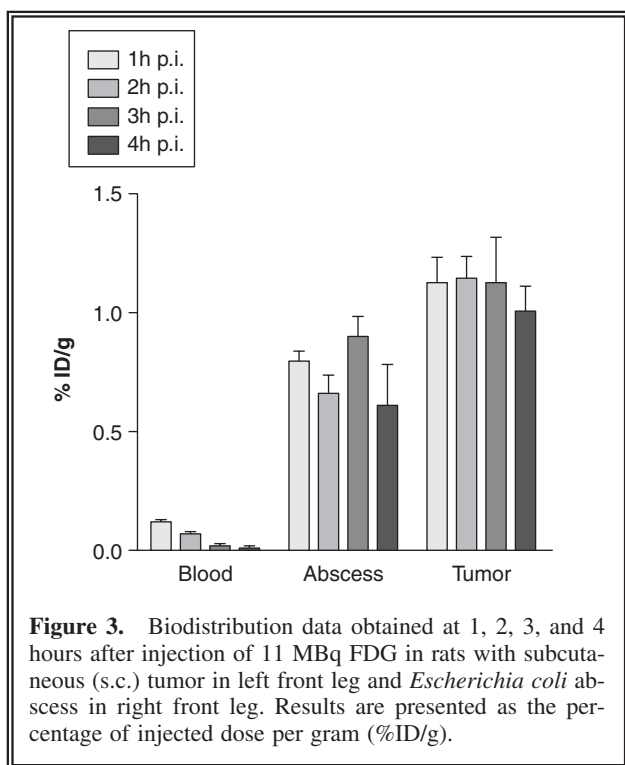

Figure 2. Data derived from ROI analysis of the PET images. Images were analyzed quantitatively by drawing regions of interest over the infected tissue and the tumor. Mean amount of activity (SUV) is represented. ROI, region of interest; PET, positron emission tomography; SUV, standardized uptake value.
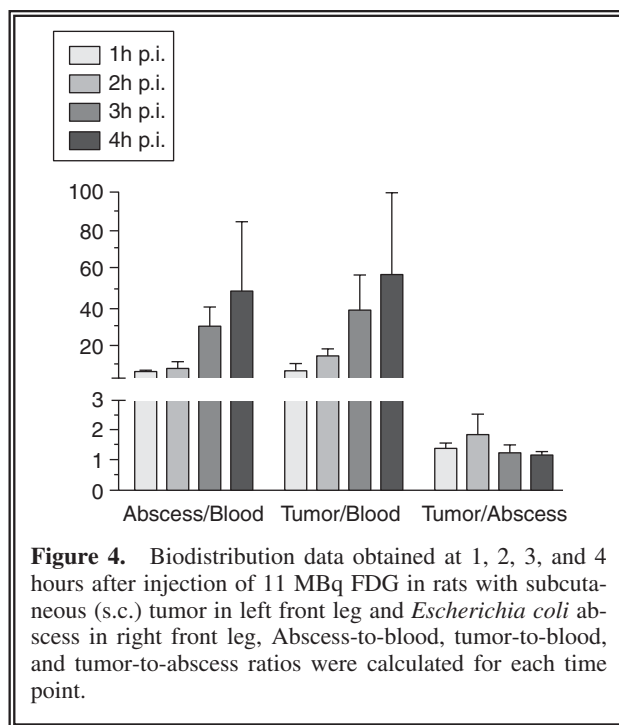
Figure 3. Biodistribution data obtained at 1, 2, 3, and 4 hours after injection of 11 MBq FDG in rats with subcutaneous (s.c.) tumor in left front leg and *Escherichia coli* abscess in right front leg. Results are presented as the percentage of injected dose per gram (%ID/g).

take in the tumor at 1 hour p.i. was 1.1 ± 0.1 %ID/g and remained stable up to 4 hours. The uptake of FDG in the abscess was 0.8 ± 0.1 %ID/g and also remained stable at that level up to 4 hours p.i. Figure 4 shows that there was a similar increase of the abscess-to-blood and the tumor-to-blood ratios. The tumor-to-blood and abscess-to-blood ratio increased with time to 57 ± 17 and 48 ± 14, respectively. Tumor-to-abscess ratios were constant.

DISCUSSION

A wide variety of tumor cells, as well as activated inflammatory cells, have an increased metabolic activity. In malignant cells, increased FDG uptake is caused by an increased glucose metabolism. This results in an upregulation of glucose transporters and glycolytic enzymes. Cells involved in the host defense against infection (e.g., infiltrating neutrophic granulocytes and tissue macrophages) have a high glucose metabolism and increased glucose uptake when activated by infection.[3,4] These pathophysiological features cause that both tumor lesions and inflammatory lesions are detected by FDG-PET. The accumulation of FDG in inflammatory le-

sions during FDG-PET scanning could reduce the accuracy of FDG-PET when used for staging or restaging malignant disease. Uptake in inflammatory lesion could decrease specificity when staging, and it may obscure tumor response upon restaging.

The results of this study showed that there was a difference in the kinetics of early FDG uptake in the infection and in the tumor. FDG was taken up faster in the infectious lesion than in the tumor. However, at later time points, neither continuous accumulation in the tumors nor wash-out from the infection was observed. This is in contrast with human studies, where it has been reported that tumor uptake of FDG increases for hours after injection. Hamberg et al. reported in a study of 8 patients with stage III lung caner that FDG uptake by tumor did not reach the maximum level within 5 hours after injection.[15] Nakamoto et al.[9] reported in a study with 47 patients with suspected pancreatic carcinoma that the retention index for malignant disease was significantly greater than that of benign disease. Zuang et al. reported that addition of a later imaging time point could aid in differentiating benign and malignant lesions.[5] The pathophysiological explanation for different FDG uptake patterns over time between inflammatory and malignant lesions is based on differences in enzyme activ-

Figure 4. Biodistribution data obtained at 1, 2, 3, and 4 hours after injection of 11 MBq FDG in rats with subcutaneous (s.c.) tumor in left front leg and *Escherichia coli* abscess in right front leg, Abscess-to-blood, tumor-to-blood, and tumor-to-abscess ratios were calculated for each time point.

ity in tumor cells and in activated leukocytes. FDG is transported into cells by glucose-transporter molecules (GLUT 1–5). The GLUT expression and its relation to FDG accumulation in malignant tumors have been investigated in clinical and experimental studies.[16] Significantly elevated expression levels of GLUT-1 and GLUT-3 are considered to be a factor contributing to the accumulation of FDG in malignant tumors. To our knowledge, the expression of GLUT receptors in our tumor model has not been studied. Mochizuki et al.[16] showed, in an animal model, a relation between FDG uptake and the expressions of GLUTs. The GLUT-1 expression level was significantly higher in the tumor lesion than in the inflammatory lesion, which may explain higher FDG accumulation in the tumor lesion. In the cell, FDG is phosphorylated to FDG-6-phosphate by hexokinase (generally, type II). FDG-6-phosphate cannot cross the cell membrane, while dephosphorylation of FDG by glucose-6-phosphatase occurs relatively slowly.[17] Thus, FDG-6-phosphate is trapped in the cells. Many cancer cells are reported to have low levels of glucose-6-phosphatase.[5] In contrast, mononuclear cells express high levels of glucose-6-phosphatase. Therefore, there might be a different ratio of hexokinase/phosphatase activity between inflammatory and malignant cells, which may result in enhanced wash-out of FDG from inflammatory cells. The relatively high glucose-6-phosphatase activity in inflammatory cells has been observed in mononuclear cells, while in acute infection the infiltrated cells are mainly granulocytes. This may explain the differences between our study (using an acute model of infection) and data in literature.[8] An interesting point for future studies would be to investigate the FDG uptake with the time of acute and chronic stage of infection.

CONCLUSIONS

This animal model showed initial differences between initial FDG uptake in tumor and acute infection with stable FDG concentrations in both lesions at later time points. FDG uptake and intracellular processing is multifactorial (e.g., dependent on vascularization, glucose transporters, intracellular glycolytic enzyme patterns, glycolytic pathways, and hypoxia). Assessment of FDG-kinetics offers a possibility to increase specificity for the differentiation between tumor and inflammation to avoid unjustified denomination of malignant lesions as benign, inflammatory tissue changes.

REFERENCES

1. Jerusalem G, Hustinx R, Beguin Y, et al. PET scan imaging in oncology. *Eur J Cancer* 2003;39:1525.
2. *Atlas of Clinical Positron Emission Tomography*, 2nd ed. Maisey MN, Wahl RL, Barrington S, eds. London: Hodder & Stoughton Educational, 1999.
3. Rennen HJ, Boerman OC, Oyen WJG, et al. Imaging infection/inflammation in the new millennium. *Eur J Nucl Med* 2001;28:241.
4. Stumpe KD, Dazzi H, Schaffner A, et al. Infection imaging using whole-body FDG-PET. *Eur J Nucl Med* 2000;27:822.
5. Zhuang H, Pourdehnad M, Lambright ES, et al. Dual time point ^{18}F-FDG-PET imaging for differentiating malignant from inflammatory processes. *J Nucl Med* 2001;42:1412.
6. Dimitrakopoulou-Strauss A, Strauss JG, Heichel T, et al. The role of quantitative ^{18}F-FDG-PET studies for the differentiation of malignant and benign bone lesions. *J Nucl Med* 2002;43:510.
7. Hustinx R, Smith RJ, Benard F, et al. Dual time point fluorine-18 fluorodeoxyglucose positron emission tomography: A potential method to differentiate malignancy from inflammation and normal tussue in the head and neck. *Eur J Nucl Med* 1999;26:1345.
8. Carsten O, Sahlmann, Ursula Siefker, et al. Dual time point [^{18}F]fluoro-2′-deoxyglucose positron emission tomography in chronic bacterial osteomyelitis. *Nucl Med Comm* 2004;25:819.
9. Nakamoto Yuji, Higashi Tatsuya, Tamaka Nagara, et al. Delayed ^{18}F-fluoro-2deoxy-D-glucose positron emission tomography scan for differentiation between malignant and benign lesions in the pancreas. *Cancer* 2000;89:2547.
10. Higashi T, Saga T, Nakamoto Y, et al. Relationship between retention index in dual-phase ^{18}F-FDG-PET, and hexokinase-II and glucose transporter-1 expression in pancreatic cancer. *J Nucl Med* 2002;43:173.
11. Ma SY, See LC, Lai CH, et al. Delayed ^{18}F-FDG-PET for detection of paraaortic lymph node metastasis in cervical cancer patients. *J Nucl Med* 2003;44:1775.
12. Matthies A, Hickeson M, Cuchiara A, et al. Dual time point ^{18}FDG-PET for the evaluation of pulmonary nodules. *J Nucl Med* 2002;43:871.
13. Stein TN, Berger MR. Quantification of liver metastases from LS174T human colorectal cancer cells in nude rats by PCR. *Anticancer Res* 1999;19:3939.
14. Kato T, Hikosaka K, Hosokawa M, et al. Effects of insulin and glucose loading on FDG uptake in experimental malignant tumors and inflammatory lesions. *Nucl Med Biol* 2004;31:875.

15. Hamberg LM, Hunter GJ, Alpert NM, et al. The dose uptake ratio as index of glucose metabolism: Use parameter or oversimplification? *J Nucl Med* 1994;35: 1308.

16. Mochizuki T, Tsukamoto E, Kuge Y, et al. FDG uptake and glucose transporter subtype expressions in experimental tumor and inflammation models. *J Nucl Med* 2001;42:1551.

17. Caraco C, Aloj L, Chen LY, et al. Cellular release of [18F]2-fluoro-2-deoxyglucose as function of the glucose-6-phosphatase enzyme system. *J Biol Chem* 2000;24:18489.

This article has been cited by:

1. Jun Toyohara, Kiichi Ishiwata. 2011. Animal tumor models for PET in drug development. *Annals of Nuclear Medicine* . [CrossRef]
2. Michael S. Hofman, Michael O#Doherty. 2007. How do we best balance optimal timing of FDG PET–CT imaging?. *Nuclear Medicine Communications* **28**:12, 885-887. [CrossRef]
3. Masatoyo Nakajo, Seishi Jinnouchi, Hiroaki Tanabe, Rie Tateno, Masayuki Nakajo. 2007. 18F-Fluorodeoxyglucose Positron Emission Tomography Features of Idiopathic Retroperitoneal Fibrosis. *Journal of Computer Assisted Tomography* **31**:4, 539-543. [CrossRef]
4. Yoshimasa Hamazawa, Koichi Koyama, Terue Okamura, Yasuhiro Wada, Tomoko Wakasa, Tomohisa Okuma, Yasuyoshi Watanabe, Yuichi Inoue. 2007. Comparison of dynamic FDG-microPET study in a rabbit turpentine-induced inflammatory model and in a rabbit VX2 tumor model. *Annals of Nuclear Medicine* **21**:1, 47-55. [CrossRef]